ORIGINAL ARTICLE

Oligomeric and fibrillar species of β-amyloid (Aβ42) both impair mitochondrial function in P301L tau transgenic mice

**Anne Eckert · Susanne Hauptmann · Isabel Scherping ·
Jessica Meinhardt · Virginie Rhein · Stefan Dröse ·
Ulrich Brandt · Marcus Fändrich · Walter E. Müller ·
Jürgen Götz**

Abstract We recently provided evidence for a mitochondrial dysfunction in P301L tau transgenic mice, a strain modeling the tau pathology of Alzheimer's disease (AD) and frontotemporal dementia (FTD). In addition to tau aggregates, the AD brain is further characterized by Aβ peptide-containing plaques. When we addressed the role of Aβ, this indicated a synergistic action of tau and Aβ pathology on the mitochondria. In the present study, we compared the toxicity of different Aβ42 conformations in light of recent studies suggesting that oligomeric rather than fibrillar Aβ might be the actual toxic species. Interestingly, both oligomeric and fibrillar, but not disaggregated (mainly monomeric) Aβ42 caused a decreased mitochondrial membrane potential in cortical brain cells obtained from FTD P301L tau transgenic mice. This was not observed with cerebellar preparations indicating selective vulnerability of cortical neurons. Furthermore, we found reductions in state 3 respiration, the respiratory control ratio, and uncoupled respiration when incubating P301L tau mitochondria either with oligomeric or fibrillar preparations of Aβ42. Finally, we found that aging specifically increased the sensitivity of mitochondria to oligomeric Aβ42 damage indicating that oligomeric and fibrillar Aβ42 are both toxic, but exert different degrees of toxicity.

A. Eckert (✉) · V. Rhein
Neurobiology Laboratory, Psychiatric University Clinic Basel,
Wilhelm Klein-Strasse 27,
4025 Basel, Switzerland
e-mail: anne.eckert@upkbs.ch

S. Hauptmann · I. Scherping · W. E. Müller
Department of Pharmacology, ZAFES, Biocenter,
University of Frankfurt am Main,
Frankfurt am Main, Germany

J. Meinhardt
Leibniz Institute for Age Research,
Jena, Germany

S. Dröse · U. Brandt
Molecular Bioenergetics Group, Centre of Biological Chemistry
and Excellence 'Macromolecular Complexes',
University Hospital Frankfurt am Main,
Frankfurt am Main, Germany

M. Fändrich
Max-Planck Research Unit for Enzymology of Protein Folding,
Martin Luther University Halle-Wittenberg,
Halle, Germany

J. Götz
Alzheimer's and Parkinson's Disease Laboratory,
Brain & Mind Research Institute, University of Sydney,
Sydney, Australia

Introduction

β-Amyloid (Aβ)-containing plaques and tau-containing neurofibrillary tangles (NFTs) are hallmarks for brain lesions in both familial and sporadic cases of Alzheimer's disease (AD); however, how these lesions and their proteinaceous components impair cellular functions and ultimately lead to

neuronal cell loss is only partly understood [1–3]. Attempts to gain insight into pathogenic mechanisms, and eventually, to develop therapeutic strategies have been greatly assisted by experimental animal models that express mutant forms of AD-associated genes [4, 5].

In AD, pathogenic mutations have been identified in both the gene encoding the precursor of the Aβ peptide, *APP*, itself and in the *PSEN* genes which encode part of the APP–protease complex. No mutations have been identified in the *MAPT* gene encoding the microtubule-associated protein tau [5]. Although AD is the most prevalent form of dementia at high age, NFTs are, in the absence of Aβ plaques, also abundant in additional neurodegenerative diseases, including frontotemporal dementia (FTD). In familial cases of FTD (FTD with Parkinsonism linked to chromosome 17 (FTDP-17)), exonic and intronic mutations have been identified in the *MAPT* gene which lead to the formation of tau aggregates in the brain [6]. Gallyas silver impregnation techniques are frequently employed to visualize NFTs in both AD and FTD brains [7].

The P301L tau mutation was among the first to be identified in FTDP-17 [8]. It was expressed by us in neurons of transgenic mice [9]. P301L tau transgenic mice develop NFTs that contain aggregated forms of hyperphosphorylated tau and show age-related memory impairment [10, 11]. Whereas transgenic mice expressing human APP with mutations found in familial cases of AD develop Aβ plaques, they fail to form NFTs. On the other hand, the P301L transgenic pR5 mice model aspects of the tau pathology of AD and FTD, but lacks plaque pathology. Both pathologies have been successfully combined either by crossing the respective transgenic strains or by establishing so-called triple transgenic mice [12] (reviewed in [13]). We addressed the pathogenic relationship of Aβ plaques and NFTs by an alternative approach that is by injecting fibrillar preparations of Aβ42 stereotaxically into the somatosensory cortex and the hippocampus of P301L and wild-type human tau transgenic mice and non-transgenic littermate controls. As shown previously, this caused a fivefold increase of NFTs in the amygdala of P301L transgenic, but not wild-type tau transgenic or control mice [14]. NFT formation was correlated with the phosphorylation of the pS422 and AT100 epitopes of tau [9, 15]. These findings could be confirmed by us in vitro, using neuronally differentiated SH-SY5Y neuroblastoma cells [16].

Subsequently, in addition to transcriptomic approaches [17, 18], we performed a proteomic and functional analysis of P301L tau transgenic mice which revealed a mitochondrial dysfunction together with a reduced electron transport chain complex I activity [19]. We also provided first evidence for an increased vulnerability of P301L tau mitochondria towards fibrillar Aβ insult, suggesting a synergistic action of tau and Aβ pathology on the mitochondria [19–21].

In recent years, attempts have been undertaken to identify the toxic species of Aβ. The focus of attention has since shifted from fibrillar to oligomeric species as the large, insoluble Aβ deposits which form the amyloid plaques in the limbic and association cortices of AD patients are in equilibrium with small, diffusible Aβ oligomers that appear capable of interfering with hippocampal synaptic function and memory [22]. Thus, in this study, we determined whether oligomeric Aβ42 would already exert a pronounced toxicity towards P301L tau transgenic mitochondria, compared to disaggregated (mainly monomeric) and fibrillar Aβ.

Materials and methods

Transgenic mice

The transgenic mice used in the present study express the human pathogenic mutation P301L of tau together with the longest human brain tau isoform (htau40) under control of the neuron-specific mThy1.2 promoter [9]. The htau40 isoform contains exons 2 and 3 as well as four microtubule-binding repeats (2^+3^+4R, human tau40). Pronuclear injections were done into C57Bl/6 × DBA/2 F2 oocytes to obtain founder animals that were back-crossed with C57Bl/6 mice to establish transgenic lines as described [23]. P301L tau mice show tau hyperphosphorylation already at 3 months [9]. NFT formation starts at 6 months of age [14]. Consistent with our previous studies [19], the mice were analyzed at 13–15 and 21–22 months of age. The mice were maintained in a 12-h dark–light cycle with pelleted food and water ad libitum. Animals were handled according to the Swiss guidelines for animal care. The experiments were conducted in accordance with international standards on animal welfare as well as being compliant with local regulations.

Monomer, oligomer, and fibril preparation

The Aβ42 synthetic peptide (H-1368, Bachem, Bubendorf, Switzerland) was suspended in 100% 1,1,1,3,3,3 hexafluoro-2-propanol (HFIP) at 6 mg/ml and incubated for complete solubilization under shaking at 37°C for 1.5 h as described previously [24].

Monomeric preparation [24] To obtain the monomeric preparation, 30 mg HFIP-treated Aβ42 was resuspended in 132 μl dimethylsulfoxide (DMSO) at RT for 10 min. A 60 ml buffer (20 mM NaPi, 140 mM NaCl, and 0.1% Pluronic F68 pH 7.4) was added and the mixture stirred for 1 h at RT. Following a 20 min centrifugation at 3,000×*g*, the supernatant was discarded and the pellet resuspended in

6 ml buffer. Then, 34 ml of H_2O was added and the mixture stirred for 1 h at RT. Following a second centrifugation for 20 min at 3,000×g, the supernatant was stored as 5 ml aliquots at −80°C.

Oligomeric preparation [24] To obtain the oligomeric preparation, HFIP was removed by evaporation in a SpeedVac and Aβ42 resuspended at a concentration of 5 mM in DMSO and sonicated for 20 s as described [16]. The HFIP-pretreated Aβ42 was diluted in phosphate-buffered saline (20 mM NaH_2PO_4, 140 mM NaCl, pH 7.4) to 400 μM and 1/10 volume 2% sodium dodecyl sulfate (SDS; in H_2O) was added (final concentration of 0.2% SDS). An incubation for 6 h at 37°C resulted in the 16/20-kDa Aβ42 globulomer (short form for globular oligomer) intermediate. The 38/48-kDa Aβ42 globulomer was generated by a further dilution with three volumes of H_2O and incubation for 18 h at 37°C. This was followed by centrifugation for 20 min at 3,000×g and concentrating the supernatant to 1.8 ml by dialysis against 5 mM NaPi, 35 mM NaCl pH 7.4 overnight at 6°C with a 30-kD centriprep and subsequent centrifugation of the concentrate for 10 min at 10,000×g. The supernatant was then stored in 100 μl aliquots at −80°C.

Fibrillar preparation adapted from previously described methods [16, 25] To prepare fibrillar Aβ42, the peptide was dissolved in Tris-buffered saline pH 7.4 (TBS) at a concentration of 0.5 mM and stored at −20°C. (All aqueous solutions were prepared with deionized and filtered water (Millipore)). The stock solution was diluted in TBS to a concentration of 50 μM and incubated at 37°C with gentle agitation for 24 h to obtain aged, aggregated preparations of Aβ42.

Visualization of Aβ preparations on sodium dodecyl sulfate polyacrylamide gel electrophoresis (SDS-PAGE) gels

The samples were analyzed using Tris-glycine 4–20% gradient SDS-PAGE gels and stained with Coomassie Brilliant Blue R250 according to [24]. Gels were scanned with an Epson 4180 scanner.

Structural characterization of Aβ aggregates

For negative staining analysis, 4 μl of the sample was placed on copper grids covered with formvar and carbon and counterstained with 2% uranyl acetate, using the droplet technique [26]. Specimens were examined in a Zeus 902 transmission electron microscope operated at an acceleration voltage of 80 kV.

Thioflavine T (ThT) spectra were recorded at room temperature with a Shimadzu RF-5301PC fluorimeter, using an excitation wavelength of 482 nm and a cuvette with 5 mm path length. Samples contained a final concentration of 20 μM ThT and 5 μM Aβ42 in 5 mM NaPi/35 mM NaCl, pH 7.4 (globulomers) or TBS, pH 7.4 (fibrils).

Congo Red (CR) absorption spectra were recorded at room temperature, using an Analytik Jena Specord 210 spectrophotometer. Samples contained a final concentration of 10 μM CR and 15 μM Aβ42 in 5 mM NaPi/35 mM NaCl, pH 7.4 (globulomers) or TBS, pH 7.4 (fibrils).

For attenuated total reflection Fourier transform infrared (ATR-FTIR) spectroscopy, Aβ42 fibrils were concentrated by centrifugation for 30 min at 500,000×g and 25°C in a Beckman Optima TLX ultracentrifuge, using a Beckman TLA-120.2 rotor. Subsequently, the fibril pellet was resuspended in a small volume of TBS, pH 7.4 by pipetting and vortexing. ATR-FTIR spectra of 1.9 mM Aβ42 globulomers in 5 mM NaPi/35 mM NaCl, pH 7.4 and 1.1 mM Aβ42 fibrils in TBS, pH 7.4 were recorded as described [27].

Brain tissue preparation for mitochondrial analysis

Cellular preparations were obtained to determine the mitochondrial membrane potential (MMP) and mitochondria and to determine respiration rates as previously described [19, 25]. For that, mice (six pairs of 13–15-month-old and six pairs of 21–22-month-old hemizygous P301L tau and WT control mice) were sacrificed by decapitation and brains quickly dissected on ice. The cerebellum and one cortical hemisphere (the other hemisphere was directly used for preparation of isolated mitochondria for mitochondrial respiration) were separately minced into 1 ml of medium I (138 mM NaCl, 5.4 mM KCl, 0.17 mM Na_2HPO_4, 0.22 mM K_2PO_4, 5.5 mM glucose, 58.4 mM sucrose, pH 7.35) with a scalpel and further dissociated by trituration through a nylon mesh (pore diameter 1 mm) with a pasteur pipette. The resulting suspension, which contained both neuronal (about 72%) and glial cells (about 26%), was filtered by gravity through a fresh nylon mesh with a pore diameter of 102 μm, and the dissociated cell aggregates were washed twice with medium II (110 mM NaCl, 5.3 mM KCl, 1.8 mM $CaCl_2·H_2O$, 1 mM $MgCl_2·6 H_2O$, 25 mM glucose, 70 mM sucrose, 20 mM 4-(2-hydroxyethyl)piperazine-1-ethanesulfonic acid (HEPES), pH 7.4) by centrifugation (400×g for 3 min at 4°C). One hundred microliters of the suspension were used for protein determination. After centrifugation, cells were resuspended in 3 ml DMEM, and then aliquots of 100 μl were distributed per well in a 48-well plate for measurement of the mitochondrial membrane potential. The preparations of cerebellar and cortical cells from P301L tau transgenic mice and WT littermate controls (cross-over design) were made within 2 h under the same conditions

and in parallel and maintained at 37°C in a humidified atmosphere of 5% CO$_2$/95% air. Viability was found to be >90% using the MTT assay and trypan blue stain exclusion test. Data are expressed as fluorescence units per milligram protein.

Determination of the mitochondrial membrane potential

The membrane potential of the inner mitochondrial membrane was measured using the rhodamine 123 (Molecular Probes, Leiden, Netherlands) dye added to the cell culture medium at a final concentration of 0.4 µM for 15 min. Cells were washed twice with Hank's balanced salt solution (Sigma, Germany), and fluorescence was determined with a Victor2 multiplate reader (Perkin Elmer, Rodgau-Jügesheim, Germany) at 490/ 535 nm (Ex/Em). Loading capacity of the dye within the membrane decreases when the mitochondrial membrane potential declines after damage, e.g., exposure to Aβ42. For the secondary insult with Aβ42, cells were incubated for 4 h with the different types of preparation as described above. For this purpose, monomeric and oligomeric preparations were handled with specific care to avoid destabilization of conformation. Thus, frozen aliquots were quickly thawed and immediately diluted to the final assay concentration (maximal incubation time at 37°C for 4 h only within the nanomolar concentration range ≤100 nM). Since pre-experiments had shown that a maximum effect of fibrillar Aβ42 with regard to a reduction of MMP was reached at a concentration of 50 nM whereas 100 nM did not further decrease MMP (data not shown), the latter concentration was omitted due to limited brain material.

Preparation of isolated mitochondria

Mice were sacrificed by decapitation and one brain hemisphere was rapidly dissected on ice and washed in ice-cold buffer (210 mM mannitol, 70 mM sucrose, 10 mM HEPES, 1 mM ethylenediamine tetraacetic acid (EDTA), 0.45% BSA, 0.5 mM DTT, protease inhibitor cocktail (Complete tablets, Roche Diagnostics). After removing the cerebellum and one cortical hemisphere for the determination of the membrane potential (see above), the second cortical hemisphere was homogenized in 2 ml buffer with a glass homogenizer (10 to 15 strokes, 400 rpm) followed by centrifugation at 1,400×g for 7 min at 4°C, to remove nuclei and tissue particles. This low speed centrifugation step was repeated once with the supernatant. Then, the supernatant fraction was centrifuged at 10,000×g for 5 min at 4°C to pellet mitochondria. The resulting pellet was resuspended in 1 ml ice-cold buffer and centrifuged again at 800×g for 3 min at 4°C. Finally, the mitochondria-enriched supernatant was centrifuged at 10,000×g for 5 min at 4°C to obtain a mitochondrial fraction. This fraction was resus-

pended in 100 µl of ice-cold buffer and stored at 4°C until use, followed by determination of protein content.

Mitochondrial respiration

The rate of mitochondrial respiration was monitored at 25°C using an Oxygraph-2k system (Oroboros, Innsbruck, Austria) equipped with two chambers and DatLab software. Mitochondria (0.5 mg) were added to 2 ml of a buffer containing 65 mM sucrose, 10 mM potassium phosphate, 10 mM Tris– HCl, 10 mM MgSO$_4$, and 2 mM EDTA (pH 7.0). State 4 respiration was measured after adding 40 µl malate/ glutamate (240 mM/280 mM; assay concentration 4.8/ 5.6 mM). Then, 10 µl adenosine diphosphate (ADP; 100 mM; assay concentration 0.5 mM) was added to measure state 3 respiration. After determining coupled respiration, 1 µl carbonyl cyanide 4-(trifluoromethoxy) phenylhydrazone (FCCP, 0.1 mM; assay concentration 0.05 nM) was added to the reaction chamber, and respiration measured in the absence of a proton gradient. To inhibit complex I activity, a total volume of 3 µl (2+1 µl) rotenone (0.1 mM; final concentration 0.15 nM) was added. Then, 10 µl succinate (1 M; final concentration 5 mM) was added and complex II-dependent respiration was measured. Finally, 8 µl KCN (0.5 M; assay concentration 2 mM) was added to inhibit complex IV activity. P301L tau transgenic and WT mitochondria were measured in parallel using the same conditions (cross-over design in the two chamber system). On a routine basis, the intactness of mitochondria was confirmed by addition of cytochrome c (10 µM). To test the effect of Aβ42 on mitochondrial respiration, isolated mitochondria were exposed to different types of Aβ42 preparations (5 µM) or vehicle on ice. Then, the mitochondria suspension was added into the chamber (final concentration of Aβ42 preparation 100 nM).

Statistical analysis

Data are represented as mean ± SEM. For statistical comparison, two-way ANOVA followed by post hoc *t* test was used. Only *p* values less than 0.05 were considered statistically significant.

Results

We previously reported a mitochondrial dysfunction in P301L tau transgenic mice that is not caused by alterations in numbers of mitochondria [19]. Furthermore, in aged P301L tau mice, we had found a significantly reduced state 3 respiration, and thus markedly reduced respiratory control ratio compared to age-matched WT mice. First evidence was provided that a secondary insult with Aβ42 caused a
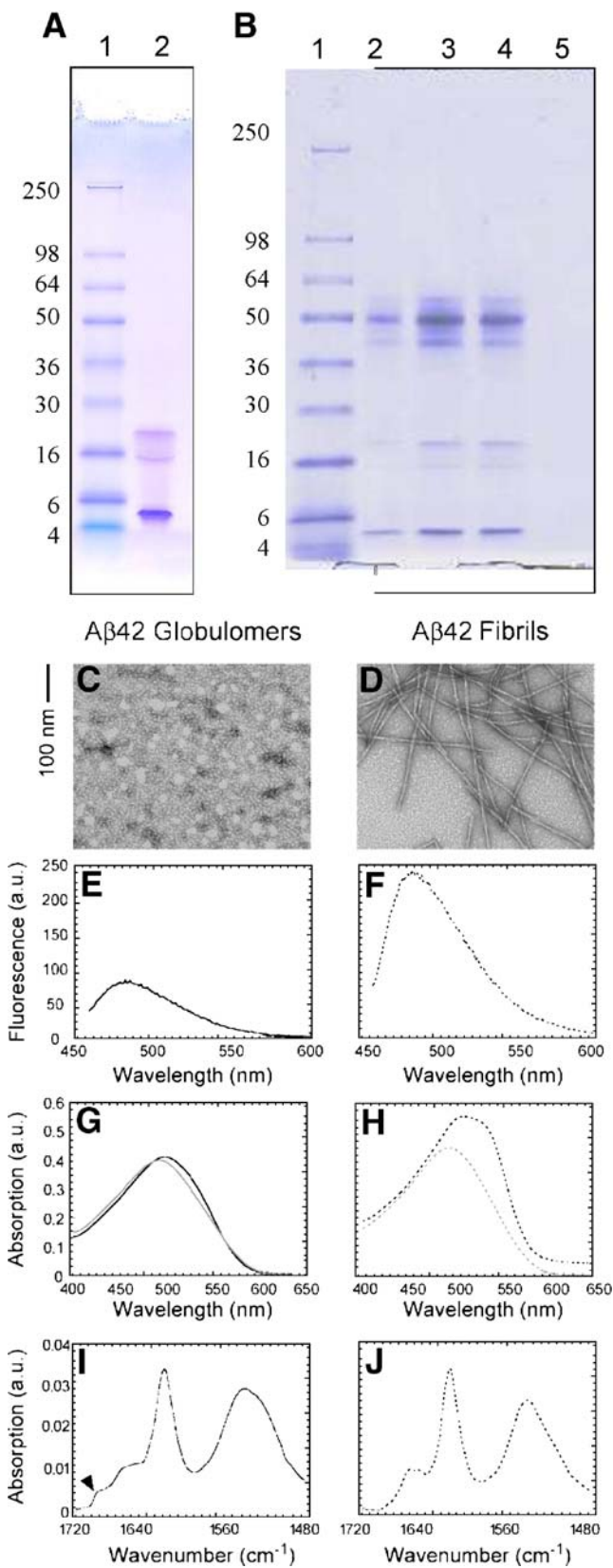
◀ **Fig. 1** Characterization of Aβ42 species. **a** Coomassie Blue-stained SDS-PAGE gel reveals predominantly monomeric Aβ42 (MW 4 kDa) in the disaggregated (monomer) preparation. The preparation does contain some heterogeneous Aβ peptides that migrate as trimers and tetramers. Lane *1* Molecular weight marker, lane *2* 5 μl of monomer preparation. **b** Characterization of the globulomer preparation. Coomassie Blue-stained SDS-PAGE gel reveals predominantly oligomeric Aβ42 (MW 50 kDa). Lane *1* Molecular weight marker, lane *2* after preparation (10 μl), lane *3* after concentration (0.5 μl), lane *4* after concentration and dialysis (0.5 μl), and lane *5* flow through (10 μl). **c, d** Electron micrographs of negatively stained Aβ42 globulomers (**c**) and fibrils (**d**) reveal spherical aggregates or mature amyloid fibrils, respectively. **e–h** ThT fluorescence emission and Congo Red absorption in the presence (*black line*) and absence (*gray line*) of globulomers (**e, g**) and fibrils (**f, h**). **i, j** ATR-FTIR spectra of Aβ42 globulomers (**i**) and fibrils (**j**). FTIR spectra were normalized to show equal intensity at the amide I′ maximum. The *arrowhead* points at the peak at 1,693 cm^{-1}, characteristic of oligomeric aggregates

higher reduction in membrane potential in P301L tau mitochondria than in WT. Here, we aimed to determine the relative toxicity of oligomeric compared to fibrillar Aβ42 with regards to mitochondrial function, by testing disaggregated (mainly monomeric), oligomeric, and fibrillar preparations of Aβ42.

Characterization of Aβ42 species

Monomeric Aβ42 was generated by an initial resuspension of Aβ42 in 1,1,3,3,3 hexafluoro-2-propanol (HFIP) followed by two centrifugation steps. The majority of the preparation was monomeric with some heterogeneous Aβ peptides that migrated on SDS-PAGE as trimers and tetramers (Fig. 1a). This preparation was, within the limits of detection, free of oligomers (no band at 50 kDa) and fibrils as confirmed by negative contrast electron microscopy (data not shown). Hence, this preparation was termed 'disaggregated'.

The oligomeric preparation with an apparent molecular weight of 50 kDa was generated by a series of concentration, centrifugation, and dialysis steps. Figure 1b shows a Coomassie Blue staining of an SDS-PAGE gel after the initial preparation of Aβ42 (10 μl, lane 2), after concentration (0.5 μl, lane 3), after concentration and dialysis (0.5 μl, lane 4), and the flow through (10 μl, lane 5). After concentrating the sample (lanes 3 and 4), the preparation mainly consisted of oligomeric Aβ42, with monomeric Aβ42 and trimers and tetramers being only a minor contaminant. Negative staining electron microscopy revealed fibril-free preparations of spherical aggregates with a diameter of 2 to 5 nm (Fig. 1c). Aβ42 globulomers bind weaker to the fluorescent amyloid-specific dye thioflavine T (ThT) compared to mature fibrils, as indicated by the smaller fluorescence intensity signal in the ThT spectrum (Fig. 1e,f). Moreover, these aggregate species do not exhibit an increased optical absorption when stained
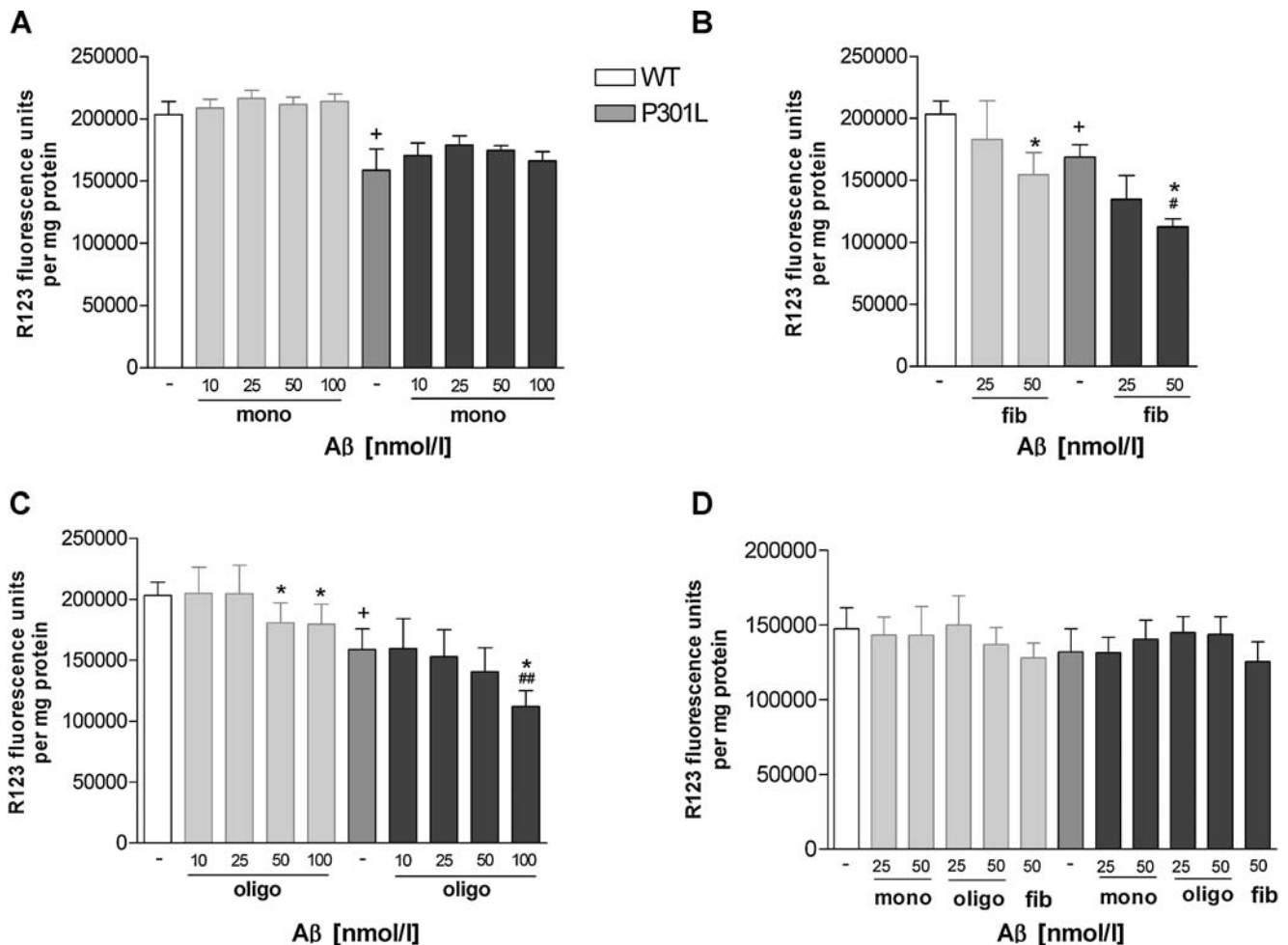
Fig. 2 Brain region-specific decrease of membrane potential after a secondary insult with either oligomeric or fibrillar, but not disaggregated (mainly monomeric), Aβ. Different preparations of Aβ42 were given to P301L tau transgenic and WT control brain cells and MMP determined using the fluorescent dye rhodamine 123. **a** Disaggregated Aβ42 added at the concentrations indicated for 4 h did not reveal differences in membrane potential between cortical brain cells of P301L transgenic and control cells. **b** Fibrillar preparations of Aβ42 caused a reduced membrane potential at 50 nmol/l for P301L tau and WT cells (*$p < 0.05$ vs. untreated corresponding control cells). P301L tau showed a significantly reduced MMP at a concentration of 50 nmol/l Aβ42 compared to WT control mice (#$p < 0.05$) as shown

with Congo Red (Fig. 1g). The FTIR spectrum of the Aβ42 globulomers provides further information on their secondary structure (Fig. 1i). The maximum of their amide I′ band is at 1,628 cm^{-1} and, therefore, within the range that is typically observed for β-sheet-rich amyloid fibrils [28]. However, the FTIR spectrum of the globulomers shows a clearly resolvable peak at 1,693 cm^{-1}, which has also been observed for Aβ40 oligomeric aggregate species and might indicate antiparallel β-sheet structure [29]. For the globulomers, the contribution of the main peak at 1,628 cm^{-1} to the amide I′ band is smaller than for Aβ42 fibrils, suggesting that they contain less β-sheet structure.

previously. Two-way ANOVA revealed a significant difference between both groups ($p < 0.05$). **c** Oligomeric (globulomeric) preparations of Aβ42 caused a reduced membrane potential at 50 and 100 nmol/l for WT cells and at 100 nmol/l for P301L tau cells (*$p < 0.05$ vs. corresponding untreated control cells). P301L tau showed a significantly reduced MMP at a concentration of 50 nmol/l oligomeric Aβ42 compared to WT control mice (##$p < 0.01$). Two-way ANOVA revealed a significant difference between both groups ($p < 0.05$). **d** Different from the cortical preparations, cerebellar preparations obtained from P301L mice are resistant to the effects of all forms of Aβ42. **a–d** Values represent means ± SE from $n = 5$–6 animals per group. All experiments were performed in duplicates

Natural human Aβ oligomers are formed soon after generation of the peptide within specific intracellular vesicles and are subsequently secreted from the cell [30]. Previous studies have shown that these Aβ42 globulomers, as they have been also termed, are a persistent structural entity formed independently of the fibrillar aggregation pathway [24]. These preparations are a potent antigen in mice and rabbits eliciting the generation of Aβ42 globulomer-specific antibodies that do not cross-react with the full-length amyloid precursor protein APP, Aβ40, and Aβ42 monomers or Aβ fibrils. Furthermore, Aβ42 globulomers have been shown to bind specifically to

dendritic processes of neurons but not glia in primary hippocampal cultures and to completely block long-term potentiation (LTP) in rat hippocampal slices [30].

Fibrillar Aβ42 was obtained by resuspension of Aβ42 in TBS and an incubation at 37°C for 24 h as described [16, 25]. Negative staining electron microscopy clearly shows mature, twisted Aβ42 fibrils with a width of 6 to 12 nm (Fig. 1d). Aβ42 fibrils show amyloid-typical tinctorial properties upon binding to ThT and CR (Fig. 1f,h). The fluorescence intensity of ThT at 482 nm and the CR absorption increase substantially in the presence of Aβ42 fibrils. Moreover, the maximum of the CR absorption is shifted from 497 to 513 nm, as typically observed for amyloid fibrils [29]. The amide I′ band of the fibrils also has its maximum at $1,628$ cm^{-1} and suggests the presence of an amyloid-like extended β-sheet structure in Aβ42 fibrils (Fig. 1j). Within the limits of detection, this preparation was free of oligomers (data not shown).

Both oligomeric and fibrillar Aβ42 cause a decreased membrane potential in P301L tau cortical preparations

We dissected the cerebellum and two cerebral brain hemispheres from 6 P301L transgenic and six non-transgenic control WT littermates at 13–15 months of age. The cerebellum and one cerebral hemisphere were triturated separately to obtain cellular preparations to determine the mitochondrial membrane potential. The second cerebral hemisphere was used to prepare isolated mitochondria to determine the rate of mitochondrial respiration. Brain cells and isolated mitochondria from the same animals were treated in parallel with the different Aβ42 preparations.

Basal MMP of cortical brain cells was already reduced in 13–15-month-old P301L tau compared to WT mice (+$p<$0.05; Fig. 2a). Treatment of cortical preparations with monomeric Aβ42 at a concentration ranging from 0 to 100 nmol/l had no effect on the MMP when P301L tau preparations were compared with non-transgenic WT littermate controls (Fig. 2a). In contrast, 50 nmol/l of fibrillar Aβ42 induced a marked impairment for both the wild-type and P301L neuronal preparations (Fig. 2b). Consistent with our previous findings [12], the Aβ42 insult resulted in a higher reduction in MMP in P301L tau mitochondria compared to WT (#$p \leq$0.05; Fig. 2b). When we tested oligomeric preparations, these had a marked effect on the MMP. WT preparations showed a reduced MMP with 50 and 100 nmol/l of oligomeric Aβ42. Cortical preparations from P301L mice showed an even more pronounced reduction of the MMP at 100 nmol/l (Fig. 2c). Again, P301L mitochondria showed a significantly reduced MMP compared to that of WT mitochondria after treatment with 100 nmol/l of oligomeric Aβ42 (##$p<$0.01; Fig. 2b).

We conclude from this that cortical preparations of both WT and P301L tau transgenic mice are susceptible to Aβ42 preparations, be they oligomeric or fibrillar in nature. Importantly, when we looked at cerebellar preparations, they were resistant to all three types of Aβ42 preparations in as much as they showed no impairment of the MMP (Fig. 2d). This finding underscores the concept of selective vulnerability in neurodegeneration. For example, for the Aβ-associated pathology in AD, five phases have been defined, with only the final fifth phase being characterized by Aβ deposition in the cerebellum [31, 32]. Similarly, NFTs are found in the cerebellum only in the final stages of AD, and in FTD, they are also not frequently encountered [33]. The mechanisms underlying selective vulnerability in AD and FTD are largely unknown, and several hypotheses have been put forward. Interestingly, one of the factors determining which cells die first when different types of cells are exposed to the same stress may be variations in mitochondrial composition [34].

Reduced state 3 respiration, respiratory control ratio, and uncoupled respiration in P301L tau mice

We have previously shown a significantly reduced state 3, but not state 4, respiration in aged (24-month-old) P301L tau transgenic compared to age-matched WT mice; this led to a markedly reduced respiratory control ratio [19].

In the present study, we restricted our analysis to the effects of oligomeric and fibrillar Aβ, determining state 3 and 4 respiration, the respiratory control ratio, and uncoupled respiration. The addition of malate and glutamate to coupled brain mitochondria, which fuel the mitochondrial NADH-generating system, allowed the analysis of the complex I-dependent respiration (Fig. 3a,b). State 3 respiration measures the capacity of mitochondria to metabolize oxygen and the selected substrate in the presence of a limited quantity of ADP, which is a substrate for adenosine triphosphate (ATP) synthase (complex V). State 4 respiration measures respiration when all ADP is exhausted and is associated with proton leakage across the inner mitochondrial membrane. Therefore, it represents a "basal-coupled" rate of respiration. We found that whereas state 4 respiration remained unchanged with NADH-generating substrates in P301L tau mice and WT controls (Figs. 3b and 4a), a significantly reduced state 3 respiration could be observed in cortical mitochondria of 13–15-month-old P301L tau mice treated with Aβ42 (Figs. 3b and 4b). Consistent with our MMP findings, WT mitochondria exhibited a reduced sensitivity to Aβ42 insults compared to P301L mitochondria (two-way ANOVA $p<$0.05). State 3 respiration was significantly reduced after treatment with oligomeric Aβ42. A similar trend was also seen after exposure to Aβ42 fibrils. We have previously shown that
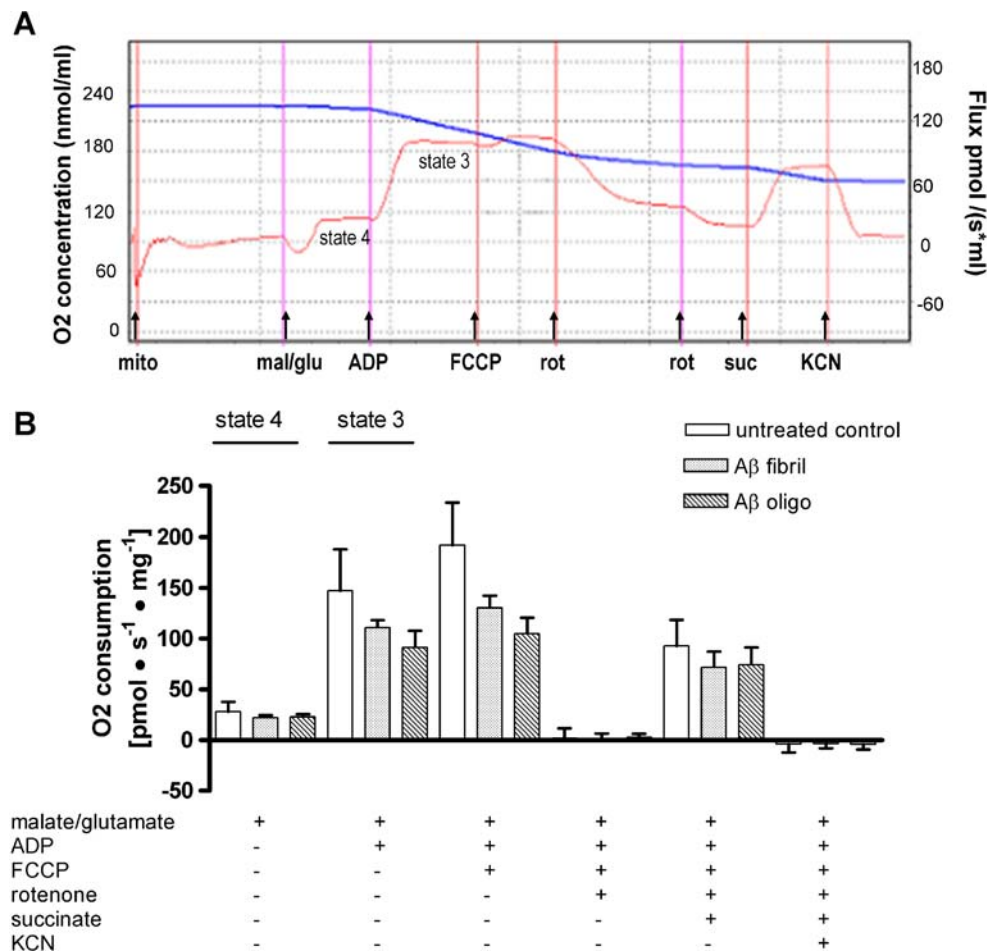
Fig. 3 Respiration of mitochondria isolated from cortical brain cells of P301L tau mice upon exposure to different Aβ preparations using an oxygen electrode. **a** Representative diagram of measurement of oxygen (O₂) consumption in mitochondria from a 15-month-old P301L tau mouse demonstrating a decrease in the total O₂ concentration with time. **b** Isolated mitochondria from 13- to 15-month-old mice were exposed to different preparations of Aβ. Then, mitochondria were added to the chamber and oxygen (O₂) flux and consumption by mitochondria (*mito*) was measured after adding different agents (marked by *arrows*): malate/glutamate (*mal/glu*; state 4), ADP (state 3), FCCP, rotenone (*rot*), succinate (*suc*), and KCN.

State 4 was measured after adding malate/glutamate. Then, ADP was added to measure state 3 respiration. After determining coupled respiration, FCCP was added and respiration was measured in the absence of a proton gradient. To inhibit complex I activity, rotenone was added. Then, respiration was measured after adding succinate. Finally, complex IV activity and O₂ consumption was inhibited by treatment with KCN. Two-way ANOVA reveals a reduced state 3 and uncoupled respiration in the presence of either fibrillar or oligomeric Aβ42 ($p<0.05$) Values represent means ± SE from $n=5$–6 animals per group. All experiments were performed in duplicates

state 3 respiration is reduced in cortical P301L tau mitochondria compared to WT controls reflecting reduced complex I activity [19]. Thus, our data indicate that the effect exerted by the presence of the P301L tau transgene on state 3 respiration is exacerbated by Aβ42. The respiratory control ratio is the ratio of state 3 to state 4 respiration, providing a measure for the efficiency of coupling of the mitochondrial respiratory chain. The respiratory control ratio is reduced in P301L tau mice treated with either oligomeric or fibrillar Aβ42 indicating that the relative efficiency of metabolic coupling of the electron chain complexes is impaired by both types of Aβ42 preparations (Fig. 4c).

We found in addition, after uncoupling with FCCP, that the respiratory rate in the absence of a proton gradient, i.e., the 'uncoupled respiration', was significantly diminished in 13–15-month-old P301L tau mice after incubation with either oligomeric or fibrillar preparations of Aβ42 (Figs. 3b and 4d) indicating a reduced maximum capacity of the electron transport chain. After complete inhibition of complex I with rotenone, succinate was added as a substrate for complex II. When the succinate-dependent respiration was normalized to the uncoupled complex I-dependent respiration in the respective experiments, there was no significant difference between treated and untreated P301L tau transgenic mitochondria (Fig. 3b). This indicates that
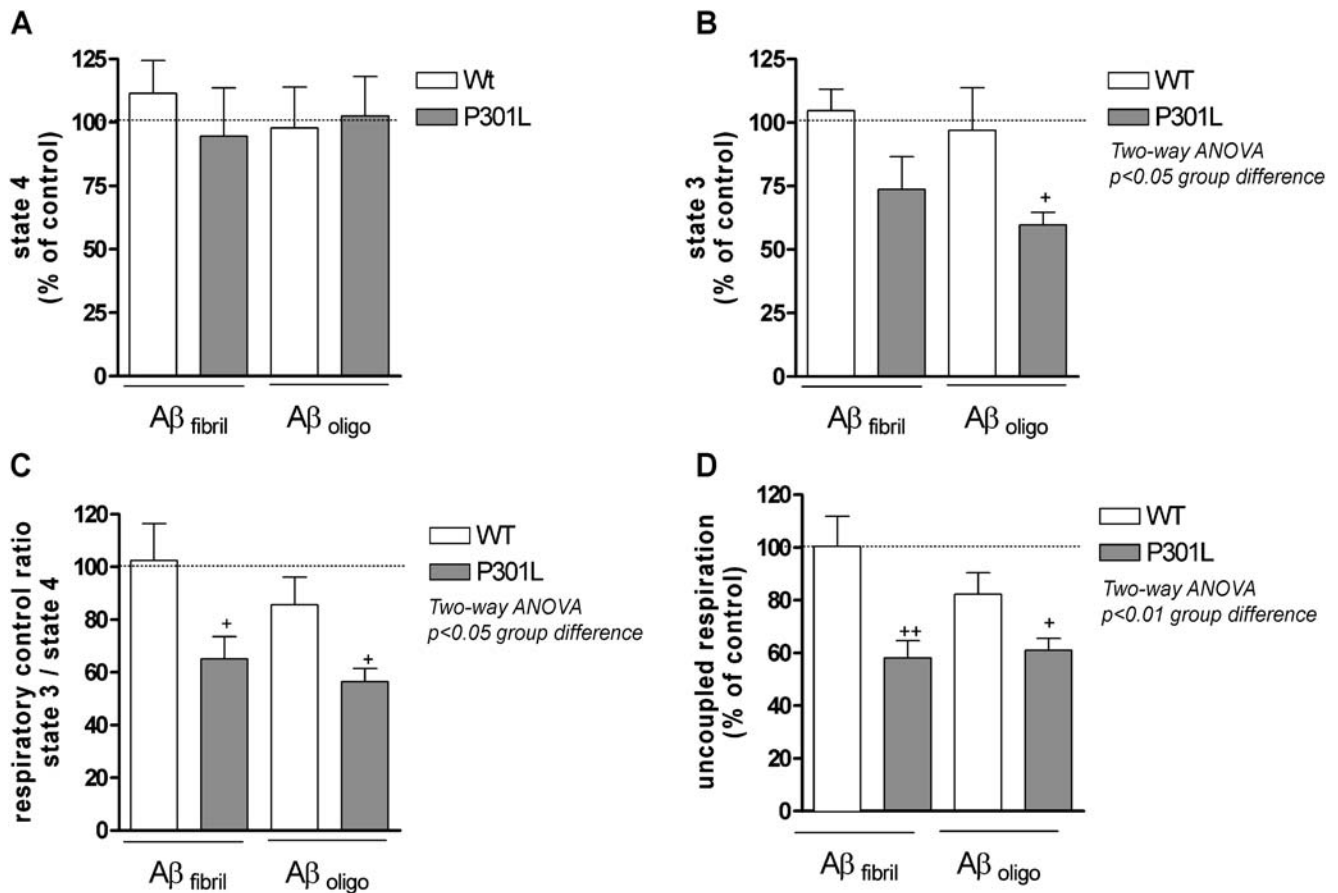
Fig. 4 Reduced state 3 respiration, RCR (respiratory control ratio), and uncoupled respiration in P301L tau mice. **a** In mitochondria from 13- to 15-month-old P301L tau transgenic mice, neither fibrillar nor oligomeric preparations of Aβ42 cause reductions of state 4 respiration. **b** State 3 respiration, however, was significantly reduced after treatment with oligomeric Aβ42 in P301L tau cells ($+p<0.05$). Two-way ANOVA reveals a significant difference between both groups with regard to the vulnerability of mitochondria to the damaging effects of Aβ42 ($p<0.05$) that is significantly increased in P301L tau mice. **c** Reduced respiratory control ratio in 13–15-month-old P301L tau mitochondria indicating an impaired efficiency of electron transport in the presence of either oligomeric or fibrillar Aβ42 (two-way ANOVA $p<0.05$, post hoc testing revealed $+p<0.05$ vs. WT). **d** Reduced uncoupled respiration in 13–15-month-old P301L tau mitochondria in the presence of either oligomeric or fibrillar Aβ42 (two-way ANOVA $p<0.01$, post hoc testing revealed $+p<0.05$ vs. oligomeric Aβ42-treated WT and $++p<0.01$ vs. fibrillar Aβ42-treated WT). **a–d** Values represent means ± SE from $n=5$–6 animals per group. All experiments were performed in duplicates

neither complex II nor complex III and IV are decisively impaired by Aβ42. In accordance with the respiratory control ratio, we have previously shown that ATP levels of cerebral cells were unchanged in 12-month-old P301L tau transgenic mice, but significantly reduced with aging [19]. Previous studies using homogenates of fresh samples of frontal neocortex from patients with dementia and neurosurgical controls suggested partial mitochondrial uncoupling in disease as the ratio of oxygen uptake rates in the presence and absence of ADP was significantly reduced for the dementia patients compared with controls [35]. These in vitro results indicate that metabolic changes may be relevant to the pathogenesis of AD and related dementias [36].

Together, our results suggest that P301L tau mice exhibit an initial defect in mitochondrial function with reduced complex I activity, which is exacerbated by the presence of either oligomeric or fibrillar Aβ42.

Aging increases the sensitivity of mitochondria to oligomeric Aβ damage

Mitochondrial respiratory chain failure has been implicated as a factor in general aging and is likely to have a greater effect in tissues with a high dependency on energy generated through oxidative phosphorylation such as the brain [37]. We have previously shown that aging contributes to the mitochondrial dysfunction in P301L tau mice [19]. Furthermore, we had found a 62.3% reduction of complex V levels in human FTDP-17 brains obtained from carriers of the P301L mutation, compared to control brains [19]. The decreased levels of complex V in human P301L
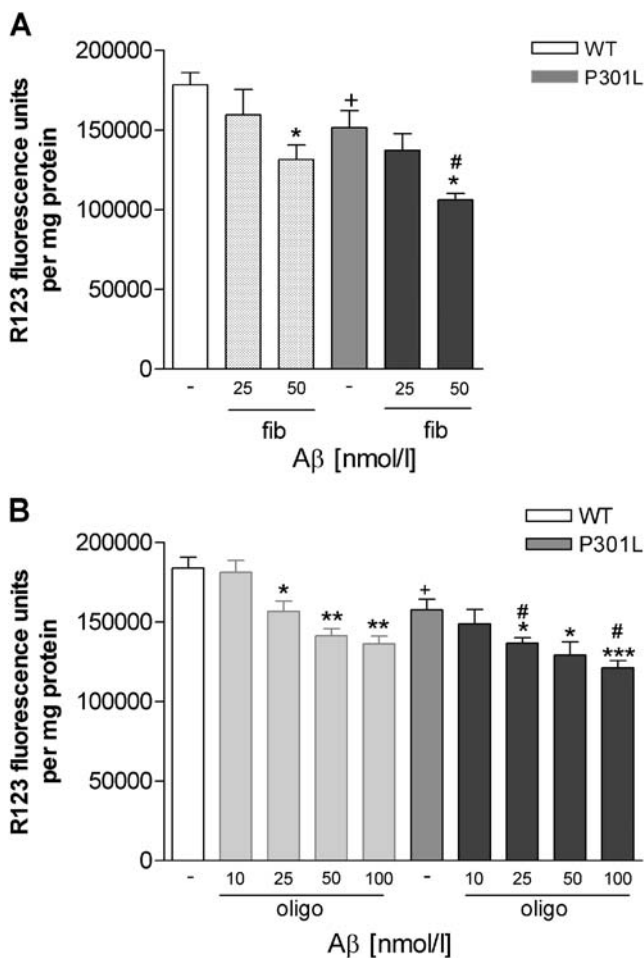
Fig. 5 Aging increases sensitivity of mitochondria to oligomeric Aβ damage. **a** For P301L tau and WT cells from 21- to 22-month-old mice, fibrillar preparations of Aβ42 cause a reduced membrane potential at 50 nmol/l (*$p<0.05$ vs. untreated corresponding control cells). P301L tau showed a significantly reduced MMP at a concentration of 50 nmol/l Aβ42 compared to WT control mice (#$p<0.05$). Two-way ANOVA revealed a significant difference between both groups ($p<0.05$). **b** Oligomeric (globulomeric) preparations of Aβ42 caused a reduced membrane potential at 25, 50, and 100 nmol/l for old WT cells and P301L tau cells from 21- to 22-month-old mice (*$p<0.05$, **$p<0.01$, ***$p<0.001$ vs. corresponding untreated control cells). P301L tau showed a significantly reduced MMP at a concentration of 25 and 100 nmol/l Aβ42 compared to WT control mice (#$p<0.05$). Two-way ANOVA revealed a significant difference between both groups ($p<0.01$). **a, b** Values represent means ± SE from $n=5-6$ animals per group. All experiments were performed in duplicates

FTDP-17 brains confirmed our proteomics observation made in the P301L tau transgenic mice and suggested that the P301L mutant tau pathology causes potentially a specific mitochondrial dysfunction in humans as well as in mice [19].

To address the toxicity of Aβ in our experimental system, we determined the MMP not only with mitochondrial preparations obtained from 13–15-month-old, but also from 21–22-month-old P301L tau transgenic mice following incubation with disaggregated (mainly monomeric), oligomeric, and fibrillar Aβ42 (Fig. 5). Again, treatment of cortical preparations with disaggregated Aβ42 at a concentration ranging from 0 to 100 nmol/l had no effect on the MMP when P301L tau preparations were compared with non-transgenic WT littermate controls (data not shown). Fibrillar Aβ42 significantly reduced MMP at a concentration of 50 nmol/l, similar to what we had found in 13–15-month-old cortical brain cells from P301L and WT mice (Fig. 5a). In contrast, oligomeric Aβ42 reduced MMP already at a concentration of 25 nmol/l in cortical WT and P301L brain cells (Fig. 5b) indicating that not the extent of mitochondrial damage but the vulnerability to Aβ42 toxicity is enhanced. Notably, cerebellar preparations did not show an age-related change in the sensitivity to all three types of Aβ42 preparations in as much as they showed no impairment of the MMP emphasizing again the concept of selective vulnerability in AD (data not shown).

Together, aging increased sensitivity of cortical mitochondria to Aβ damage. This is in agreement with studies in APP transgenic mice [25] as well as in primates, where complex I activity had been shown to be reduced with aging [38]. Thus, aging potentially intensifies complex I activity defects in the P301L tau mice.

Discussion

Our findings first of all support the notion of a toxic role of Aβ in respiration and, together with our previous findings, antioxidant defense mechanisms [19, 25, 39]. Secondly, they reveal a role for tau in mitochondrial dysfunction. Thirdly, our experiments extend our previous findings that treatment of PC12 cells with extracellular Aβ causes a significant decrease in mitochondrial membrane potential [40]. Finally, our results in P301L tau mice indicate the effects of both fibrillar and oligomeric Aβ on mitochondrial function of cortical brain cells at very low and physiological relevant concentrations within the nanomolar range and within a very short time frame (incubation time 4 h) indicating early and chronic alterations of mitochondrial functions that may impact overall neuronal homeostasis. In a related study, acute treatment of human cortical neurons with oligomeric Aβ (5 μM) for only short periods was shown to be sufficient to activate a mitochondrial apoptotic death pathway [41].

How does Aβ exert its effect on mitochondria? Interaction of Aβ with Aβ binding alcohol dehydrogenase (ABAD), a short-chain alcohol dehydrogenase in the mitochondrial matrix, has been shown to lead to mitochondria failure, e.g., mitochondrial membrane permeability and reduction of the activities of enzymes involved in mito-

chondrial respiration [42]. ABAD also binds to oligomeric Aβ42 that has been found in cortical mitochondria of APP transgenic mice [43]. Protease sensitivity assays suggest that Aβ gains access to the mitochondrial matrix rather than simply being adsorbed to the external surface of mitochondria [44]. This may explain how Aβ42 affects mitochondrial membrane potential and respiration. In our studies, however, we did not determine whether there is a direct interaction between Aβ and mitochondria, nor whether extracellular Aβ is taken up by the neurons. It is very likely that within the short time frame of our experiments (i.e., 4 h) very little Aβ42 is taken up at all. The effects of this putatively minor fraction cannot be discriminated from that elicited by the majority of Aβ that is not taken up. Therefore, our experimental design does not allow drawing any conclusions concerning the role of intracellular Aβ in mitochondrial dysfunction. In any case, it is generally not understood how Aβ exerts its toxicity in other experimental paradigms, whether it is receptor mediated and if so whether it requires uptake of Aβ by nerve terminals and retrograde transport, whether it is dependent on pore formation and calcium ion influx, or whether it is related to damage to nerve terminals, by interacting with the lipid bilayer [45]. It has been hypothesized that oligomeric Aβ, with its sharp morphology in contrast to monomeric Aβ, has the ability to permeabilize cellular membranes and lipid bilayers thereby entering organelles, such as the mitochondria [46, 47]. Of note, early reports about the action of aggregated Aβ on membranes implicate increased membrane permeability elicited by fibrils [48, 49]. These mechanisms might explain why aggregated Aβ preparations elicit effects on mitochondrial function, but not disaggregated Aβ.

The differences we found between the effects of fibrillar and oligomeric Aβ are subtle. In a related study, their effects have been dissected from monomers. Cell medium containing oligomers and abundant Aβ monomers, but not amyloid fibrils, were microinjected into rat brain and shown to markedly inhibit hippocampal long-term potentiation [30]. Immunodepletion from the medium of all Aβ species completely abrogated this effect. Pretreatment of the medium with insulin-degrading enzyme, which degrades Aβ monomers but not oligomers, did not prevent the inhibition of LTP, indicating a role for Aβ oligomers. These were shown to disrupt synaptic plasticity in vivo at concentrations found in human brain and cerebrospinal fluid, in the absence of monomeric or fibrillar amyloid. When cells were treated with γ-secretase inhibitors at doses which prevented oligomer formation but allowed appreciable monomer production, this no longer disrupted LTP, indicating that synaptotoxic Aβ oligomers can be targeted therapeutically [30, 50]. In Neuro-2A cells, oligomers were shown to induce a tenfold greater increase in neurotoxicity

as compared to fibrils [51]. However, whereas LTP seems to be inhibited by oligomeric Aβ only and not by fibrillar Aβ, in a different experimental paradigm, as in our study, the two species seem to have both toxic, yet diverse effects [52]. Using rat astrocyte cultures, oligomeric Aβ42 was shown to induce initial high levels of the pro-inflammatory molecule IL-1β that decreased over time, whereas fibrillar Aβ caused increased levels over time [52]. Oligomeric, but not fibrillar Aβ, induced high levels of iNOS, NO, and TNFα, suggesting that oligomers induce a profound, early inflammatory response, whereas fibrillar Aβ shows less increases of pro-inflammatory molecules, consistent with a more chronic form of inflammation [52]. Similarly, in our experimental paradigm, we found toxic effects of both fibrillar and oligomeric Aβ, but those of oligomeric Aβ were more pronounced.

The presence of the pathogenic P301L mutation of tau severely increased the susceptibility of mitochondria to Aβ preparations. How tau accumulation is mediating these changes is unclear. Overexpression of wild-type tau in cell culture has been shown to impair plus-end-directed axonal transport resulting in a reduction of mitochondria [53]. However, this is unlikely the case for P301L tau mice, as mitochondrial neuritic numbers counted proximal or distal to the cell body, did not vary significantly compared to numbers in WT mice, [19]. Also, the total amount of mitochondria has been shown to be unaltered in the transgenic mice [19]. This is consistent with the finding of similar numbers of mitochondria between NFT and non-NFT-bearing cells in AD [54]. It is likely that tau accumulation has direct effects on the mitochondria as the accumulation of increasingly insoluble ATP synthase α-chain together with NFTs has been shown in AD brains while detergent-soluble levels were reduced [55].

The synergistic effects of Aβ42 on mitochondria isolated from P301L tau transgenic mice may seem subtle, irrespective of whether they are incubated with fibrillar or oligomeric Aβ42, but these effects are of in vivo relevance as AD is a chronic and slowly progressive disease, with time spans of up to several decades between Aβ and tau aggregation and the onset of clinical symptoms.

In conclusion, we found that both fibrillar and oligomeric Aβ42 preparations impaired mitochondrial membrane potential and respiration. Furthermore, we revealed the synergistic effects of Aβ42 and P301L tau (see also: [56]). However, as aged cortical brain mitochondria showed an increased sensitivity to oligomeric compared to fibrillar Aβ, this suggests that oligomeric Aβ may be particularly toxic. Although it is likely that oligomeric Aβ represents the primary toxic insult, further experiments are needed to substantiate this notion. Thus, there is increasing evidence for different modes of toxic actions of Aβ suggesting that in the development of treatment strategies, targeting either

oligomeric or fibrillar Aβ may not be sufficient, but the best approach is likely one that either prevents formation of excess Aβ altogether or assists in its rapid clearance.

References

1. Diaz-Nido J, Wandosell F, Avila J (2002) Glycosaminoglycans and beta-amyloid, prion and tau peptides in neurodegenerative diseases. Peptides 23:1323–1332

2. Avila J (2006) Tau phosphorylation and aggregation in Alzheimer's disease pathology. FEBS Lett 580:2922–2927

3. Stefani M, Dobson CM (2003) Protein aggregation and aggregate toxicity: new insights into protein folding, misfolding diseases and biological evolution. J Mol Med 81:678–699

4. Gotz J, Streffer JR, David D, Schild A, Hoerndli F, Pennanen L, Kurosinski P, Chen F (2004) Transgenic animal models of Alzheimer's disease and related disorders: histopathology, behavior and therapy. Mol Psychiatry 9:664–683

5. Gotz J, Ittner LM (2008) Animal models of Alzheimer's disease and frontotemporal dementia. Nat Rev Neurosci 9:532–544

6. Lee VM, Goedert M, Trojanowski JQ (2001) Neurodegenerative tauopathies. Annu Rev Neurosci 24:1121–1159

7. Chen F, David D, Ferrari A, Gotz J (2004) Posttranslational modifications of tau-role in human tauopathies and modeling in transgenic animals. Curr Drug Targets 5:503–515

8. Hutton M, Lendon CL, Rizzu P, Baker M, Froelich S, Houlden H, Pickering-Brown S, Chakraverty S, Isaacs A, Grover A, Hackett J, Adamson J, Lincoln S, Dickson D, Davies P, Petersen RC, Stevens M, de Graaff E, Wauters E, van Baren J, Hillebrand M, Joosse M, Kwon JM, Nowotny P, Che LK, Norton J, Morris JC, Reed LA, Trojanowski J, Basun H, Lannfelt L, Neystat M, Fahn S, Dark F, Tannenberg T, Dodd PR, Hayward N, Kwok JB, Schofield PR, Andreadis A, Snowden J, Craufurd D, Neary D, Owen F, Oostra BA, Hardy J, Goate A, van Swieten J, Mann D, Lynch T, Heutink P (1998) Association of missense and 5¢-splice-site mutations in tau with the inherited dementia FTDP-17. Nature 393:702–705

9. Gotz J, Chen F, Barmettler R, Nitsch RM (2001) Tau filament formation in transgenic mice expressing P301L tau. J Biol Chem 276:529–534

10. Pennanen L, Welzl H, D'Adamo P, Nitsch RM, Gotz J (2004) Accelerated extinction of conditioned taste aversion in P301L tau transgenic mice. Neurobiol Dis 15:500–509

11. Pennanen L, Wolfer DP, Nitsch RM, Gotz J (2006) Impaired spatial reference memory and increased exploratory behavior in P301L tau transgenic mice. Genes Brain Behav 5:369–379

12. Oddo S, Caccamo A, Shepherd JD, Murphy MP, Golde TE, Kayed R, Metherate R, Mattson MP, Akbari Y, LaFerla FM (2003) Triple-transgenic model of Alzheimer's disease with plaques and tangles: intracellular Abeta and synaptic dysfunction. Neuron 39:409–421

13. Gotz J, Deters N, Doldissen A, Bokhari L, Ke Y, Wiesner A, Schonrock N, Ittner LM (2007) A decade of tau transgenic animal models and beyond. Brain Pathol 17:91–103

14. Gotz J, Chen F, van Dorpe J, Nitsch RM (2001) Formation of neurofibrillary tangles in P301l tau transgenic mice induced by Abeta 42 fibrils. Science 293:1491–1495

15. Deters N, Ittner LM, Gotz J (2008) Divergent phosphorylation pattern of tau in P301L tau transgenic mice. Eur J Neurosci 28:137–147

16. Ferrari A, Hoerndli F, Baechi T, Nitsch RM, Gotz J (2003) beta-Amyloid induces paired helical filament-like tau filaments in tissue culture. J Biol Chem 278:40162–40168

17. Chen F, Wollmer MA, Hoerndli F, Munch G, Kuhla B, Rogaev EI, Tsolaki M, Papassotiropoulos A, Gotz J (2004) Role for glyoxalase I in Alzheimer's disease. Proc Natl Acad Sci U S A 101:7687–7692

18. Hoerndli F, David DC, Gotz J (2005) Functional genomics meets neurodegenerative disorders. Part II: application and data integration. Prog Neurobiol 76:169–188

19. David DC, Hauptmann S, Scherping I, Schuessel K, Keil U, Rizzu P, Ravid R, Drose S, Brandt U, Muller WE, Eckert A, Gotz J (2005) Proteomic and functional analyses reveal a mitochondrial dysfunction in P301L tau transgenic mice. J Biol Chem 280:23802–23814

20. Hauptmann S, Keil U, Scherping I, Bonert A, Eckert A, Muller WE (2006) Mitochondrial dysfunction in sporadic and genetic Alzheimer's disease. Exp Gerontol 41:668–673

21. Eckert A, Hauptmann S, Scherping I, Rhein V, Muller-Spahn F, Gotz J, Muller WE (2008) Soluble beta-amyloid leads to mitochondrial defects in amyloid precursor protein and tau transgenic mice. Neurodegener Dis 5:157–159

22. Selkoe DJ (2002) Alzheimer's disease is a synaptic failure. Science 298:789–791

23. Ittner LM, Gotz J (2007) Pronuclear injection for the production of transgenic mice. Nat Protoc 2:1206–1215

24. Barghorn S, Nimmrich V, Striebinger A, Krantz C, Keller P, Janson B, Bahr M, Schmidt M, Bitner RS, Harlan J, Barlow E, Ebert U, Hillen H (2005) Globular amyloid beta-peptide oligomer—a homogenous and stable neuropathological protein in Alzheimer's disease. J Neurochem 95:834–847

25. Hauptmann S, Scherping I, Drose S, Brandt U, Schulz KL, Jendrach M, Leuner K, Eckert A, Muller WE (2008) Mitochondrial dysfunction: an early event in Alzheimer pathology accumulates with age in AD transgenic mice. Neurobiol Aging (in press)

26. Harris JR (1997) Negative staining and cryoelectron microscopy: the thin film techniques. Bios Scientific, Oxford

27. Hortschansky P, Schroeckh V, Christopeit T, Zandomeneghi G, Fandrich M (2005) The aggregation kinetics of Alzheimer's beta-amyloid peptide is controlled by stochastic nucleation. Protein Sci 14:1753–1759

28. Zandomeneghi G, Krebs MR, McCammon MG, Fandrich M (2004) FTIR reveals structural differences between native beta-sheet proteins and amyloid fibrils. Protein Sci 13:3314–3321

29. Habicht G, Haupt C, Friedrich RP, Hortschansky P, Sachse C, Meinhardt J, Wieligmann K, Gellermann GP, Brodhun M, Gotz J, Halbhuber KJ, Rocken C, Horn U, Fandrich M (2007) Directed selection of a conformational antibody domain that prevents mature amyloid fibril formation by stabilizing Abeta protofibrils. Proc Natl Acad Sci U S A 104:19232–19237

30. Walsh DM, Klyubin I, Fadeeva JV, Cullen WK, Anwyl R, Wolfe MS, Rowan MJ, Selkoe DJ (2002) Naturally secreted oligomers of amyloid beta protein potently inhibit hippocampal long-term potentiation in vivo. Nature 416:535–539

31. Braak H, Braak E (1991) Neuropathological staging of Alzheimer-related changes. Acta Neuropathol 82:239–259

32. Braak H, Braak E (1995) Staging of Alzheimer's disease-related neurofibrillary changes. Neurobiol Aging 16:271–278 discussion 8-84

33. Thal DR, Rub U, Orantes M, Braak H (2002) Phases of A beta-deposition in the human brain and its relevance for the development of AD. Neurology 58:1791–1800

34. Ko LW, Sheu KF, Thaler HT, Markesbery WR, Blass JP (2001) Selective loss of KGDHC-enriched neurons in Alzheimer temporal cortex: does mitochondrial variation contribute to selective vulnerability? J Mol Neurosci 17:361–369

35. Sims NR, Finegan JM, Blass JP, Bowen DM, Neary D (1987) Mitochondrial function in brain tissue in primary degenerative dementia. Brain Res 436:30–38

36. Lin MT, Beal MF (2006) Mitochondrial dysfunction and oxidative stress in neurodegenerative diseases. Nature 443:787–795

37. Ojaimi J, Masters CL, Opeskin K, McKelvie P, Byrne E (1999) Mitochondrial respiratory chain activity in the human brain as a function of age. Mech Ageing Dev 111:39–47

38. Bowling AC, Mutisya EM, Walker LC, Price DL, Cork LC, Beal MF (1993) Age-dependent impairment of mitochondrial function in primate brain. J Neurochem 60:1964–1967

39. Schuessel K, Schafer S, Bayer TA, Czech C, Pradier L, Muller-Spahn F, Muller WE, Eckert A (2005) Impaired Cu/Zn-SOD activity contributes to increased oxidative damage in APP transgenic mice. Neurobiol Dis 18:89–99

40. Keil U, Bonert A, Marques CA, Scherping I, Weyermann J, Strosznajder JB, Muller-Spahn F, Haass C, Czech C, Pradier L, Muller WE, Eckert A (2004) Amyloid beta-induced changes in nitric oxide production and mitochondrial activity lead to apoptosis. J Biol Chem 279:50310–50320

41. Deshpande A, Mina E, Glabe C, Busciglio J (2006) Different conformations of amyloid beta induce neurotoxicity by distinct mechanisms in human cortical neurons. J Neurosci 26:6011–6018

42. Lustbader JW, Cirilli M, Lin C, Xu HW, Takuma K, Wang N, Caspersen C, Chen X, Pollak S, Chaney M, Trinchese F, Liu S, Gunn-Moore F, Lue LF, Walker DG, Kuppusamy P, Zewier ZL, Arancio O, Stern D, Yan SS, Wu H (2004) ABAD directly links Abeta to mitochondrial toxicity in Alzheimer's disease. Science 304:448–452

43. Yan Y, Liu Y, Sorci M, Belfort G, Lustbader JW, Yan SS, Wang C (2007) Surface plasmon resonance and nuclear magnetic resonance studies of ABAD-Abeta interaction. Biochemistry 46:1724–1731

44. Caspersen C, Wang N, Yao J, Sosunov A, Chen X, Lustbader JW, Xu HW, Stern D, McKhann G, Yan SD (2005) Mitochondrial Abeta: a potential focal point for neuronal metabolic dysfunction in Alzheimer's disease. FASEB J 19:2040–2041

45. Jaeger S, Pietrzik CU (2008) Functional role of lipoprotein receptors in Alzheimer's disease. Curr Alzheimer Res 5:15–25

46. Glabe CG, Kayed R (2006) Common structure and toxic function of amyloid oligomers implies a common mechanism of pathogenesis. Neurology 66:S74–S78

47. Reddy PH, Beal MF (2008) Amyloid beta, mitochondrial dysfunction and synaptic damage: implications for cognitive decline in aging and Alzheimer's disease. Trends Mol Med 14:45–53

48. Simmons MA, Schneider CR (1993) Amyloid beta peptides act directly on single neurons. Neurosci Lett 150:133–136

49. Arispe N, Rojas E, Pollard HB (1993) Alzheimer disease amyloid beta protein forms calcium channels in bilayer membranes: blockade by tromethamine and aluminum. Proc Natl Acad Sci U S A 90:567–571

50. Walsh DM, Klyubin I, Shankar GM, Townsend M, Fadeeva JV, Betts V, Podlisny MB, Cleary JP, Ashe KH, Rowan MJ, Selkoe DJ (2005) The role of cell-derived oligomers of Abeta in Alzheimer's disease and avenues for therapeutic intervention. Biochem Soc Trans 33:1087–1090

51. Stine WB Jr, Dahlgren KN, Krafft GA, LaDu MJ (2003) In vitro characterization of conditions for amyloid-beta peptide oligomerization and fibrillogenesis. J Biol Chem 278:11612–11622

52. White JA, Manelli AM, Holmberg KH, Van Eldik LJ, Ladu MJ (2005) Differential effects of oligomeric and fibrillar amyloid-beta 1-42 on astrocyte-mediated inflammation. Neurobiol Dis 18:459–465

53. Ebneth A, Godemann R, Stamer K, Illenberger S, Trinczek B, Mandelkow E (1998) Overexpression of tau protein inhibits kinesin-dependent trafficking of vesicles, mitochondria, and endoplasmic reticulum: implications for Alzheimer's disease. J Cell Biol 143:777–794

54. Sumpter PQ, Mann DM, Davies CA, Neary D, Snowden JS, Yates PO (1986) A quantitative study of the ultrastructure of pyramidal neurons of the cerebral cortex in Alzheimer's disease in relationship to the degree of dementia. Neuropathol Appl Neurobiol 12:321–329

55. Sergeant N, Wattez A, Galvan-Valencia M, Ghestem A, David JP, Lemoine J, Sautiere PE, Dachary J, Mazat JP, Michalski JC, Velours J, Mena-Lopez R, Delacourte A (2003) Association of ATP synthase alpha-chain with neurofibrillary degeneration in Alzheimer's disease. Neuroscience 117:293–303

56. Hoerndli FJ, Pelech S, Papassotiropoulos A, Gotz J (2007) Abeta treatment and P301L tau expression in an Alzheimer's disease tissue culture model act synergistically to promote aberrant cell cycle re-entry. Eur J Neurosci 26:60–72